2022-11-02

Passive motion reduction of semisubmersible floating offshore wind turbine foundations

Johannesen, I

http://hdl.handle.net/10026.1/20163

10.1201/9781003360773
Trends in Renewable Energies Offshore: Proceedings of the 5th International Conference on Renewable Energies Offshore (RENEW 2022) (1st ed.)
Taylor & Francis Group

Passive motion reduction of semisubmersible floating offshore wind turbine foundations

Ignacio P. Johannesen, Edward Ransley, Martyn Hann, Shanshan Cheng & Deborah Greaves.

School of Engineering, Computing and Mathematics, University of Plymouth, Plymouth, Devon, UK.

ABSTRACT: The present work consists of numerical analysis of passive motion reduction strategies applied to semi-submersible platforms for Floating Offshore Wind (FOW) turbines. Focusing on damping structures, such as, heave plates, structures designed to damp the platforms vertical motion, by increasing the added mass and viscous damping of the device. Nevertheless, in terms of motion response, the main issue for FOW turbines is associated with pitch motion. The aim of this work is to improve understanding of heave plate influence on pitch motion, allowing for potential improvements in motion reduction in the future. The main amount of data it was obtained by NEMOH a potential flow Boundary Element Method (BEM) code. In addition, the open-source code OpenFOAM with a Reynolds-averaged Navier–Stokes equations (RANS) based solver is used to solve the flow-structure interaction of this problem and the results are compared against experimental data from the literature.

1 INTRODUCTION

Human-induced climate change, caused by excessive greenhouse gas emission, is affecting the global ecosystem. To minimize the dangers of climate change, international entities have developed long-term strategies to decarbonize the energy system, where renewable energies are the main option to reduce carbon emissions.

Wind energy has shown to be a reliable technology with great potential. The wind energy industry has moved to offshore sites to reach better wind sources with less visual and noise pollution. However, currently the most used foundation technique is by a bottom fixed structure, which is not economically viable for water deeper than 50m (James & Costa Ros, 2015). This limitation does not allow further expansion to wind farm locations in deep water.

An alternative for wind turbine foundations is to use a floating platform capable of allocate the turbine while ensuring good performance and survivability of the system. The Floating Offshore Wind Turbines (FOWT) technology is currently in an early stage, but there are some large-scale tests and accepted farm projects. Nevertheless, the lack of design convergence leads to a non-optimal design solution and therefore, to a higher levelized cost of energy (LCOE). Among the studied floating devices for FOWT, the semi-submersible platform (SSP) is highlighted for its flexibility in terms of deployment sites and the lower port-ship resources necessary for the installation, making this option one of the most studied/tested models for this application. However, compared with spar buoy or tension-leg platforms, it generally represent a higher LCOE. The work done by Lerch et al. (2018) shows that one of the best options to decrease the LCOE of SSPs is the platform design itself, where a decrease of 20% in costs can lead up to a 5% reduction in the LCOE. Myhr et al. (2014) made a CAPEX projection of FOWT, highlighting the platform as the main parameter in the system costs. These can be explained by the large mass needed to ensure stability (Maimon, 2019), in this kind of platform. Hence, an effective way to reduce the LCOE of semi-submersible FOWTs, is to reduce the size and dry mass of the device. However, this would cause stability issues, affecting the performance of the turbine. Therefore, to ensure a proper behaviour of a light-weight system under different conditions, a motion reduction strategy must be applied. Then, due to their simplicity and possible lower associated costs, a passive device such as a heave plate is studied to increase the added mass and viscous damping properties and finally reduce the response of the body, to wave and wind loads.

The influence of these properties is usually approximated via a general constant coefficient or a linear frequency dependent parameter that does not vary significantly. Nevertheless, the associated flow-structure interaction requires deeper analysis, especially when the device relies on these phenomena. Numerical tools such as Computational Fluid Dynamic

(CFD) arise as good alternatives to study these problem by solving high order hydrodynamic phenomena. As it is described in T. Sarpkaya & Isaacson (1981), these effects depend highly on time and the past history to determine the following results, here phenomena such as vortex generation and large changes in flow velocities interfere, developing substantial differences among the results of added mass and damping forces. Works such as that presented by Bayati et al. (2014) and Roald et al. (2013) show that non-linear components cannot be neglected, especially in severe sea states.

The objective of this study is to produce knowledge to enable motion reduction in heave and pitch modes of a semi-submersible platform. In order to achieve this objective, a shape variation study was performed with the Boundary Element Method (BEM) code NEMOH. In addition, a CFD study was carried out to validate and /or compare the results obtained from the more basic flow solver. In this way, it is possible to reduce the uncertainties when the proposed geometries are tested for future work.

In the literature of semi-submersible platform studies, usually the whole platform analysed. However, since a more detailed analysis of the plates behaviour is desired, and to avoid extra effects acting on the simulations, this research has been carried out with a single column geometry, with the application for a multiple column semi-submersible system.

2 THEORETICAL FORMULATION

2.1 *Hydrodynamic force coefficients*

Devices such as heave plates or others appendages to ships and platforms normally generate higher damping forces and added mass, to reduce the response of the body to exciting loads. Therefore, characterizing the performance of a disk used as a motion reduction plate is a key process to understand how the flow-structure interaction works and what improvements could be made. Keulegan & Carpenter (1958) first studied their dependency, where they showed that there is a velocity and a periodic relation to the developed inertia and damping effects. Later, this was expanded and renamed as the Keulegan & Carpenter number (KC) and Beta number (β) both related to the Reynolds number (R_e), as are shown:

$$KC = \frac{2\pi z_a}{D_d}, \quad (1)$$

$$\beta = \frac{D^2 f}{\nu} \quad (2)$$

$$R_e = KC\beta \quad (3)$$

Where, z_a is the amplitude of motion, D_d is the diameter of the disk, f is the frequency of motion and ν the kinematic viscosity of water.

The damping forces are proportional to velocity and act against the direction of motion, dissipating energy into the flow in the form of motion. A floating body, has two main forms of damping forces, the potential or wave radiation damping and the viscous damping. For floating bodies, such as ships, buoys, barges, platforms or any large floating structure, it is commonly accepted that only the wave radiation damping would be significant, due to the small magnitude of viscous damping in these cases (Journee & Massie, 2000). However, in the case of a deeply submerged heave plate that does not create substantial radiation waves, it can be considered that the damping effects are purely originated by viscous effects. The damping coefficient "b" is a parameter used to describe the damping force in terms of the velocity of the body. Here, it will be considered as a linear representation of the non-linear damping coefficient used in Morison-like forces.

The added mass "a" was defined by T. Sarpkaya & Isaacson (1981) as the quotient of the additional force required to produce the accelerations along the flow, divided by the acceleration of the body. This means that an amount of water mass moves as a reaction of the body motion, creating a system with a higher virtual mass. In this work, two different methods are used to obtain these parameters, CFD simulation of a forced oscillating motion (FOM) test and a BEM. The basic theory about these methods will be explained in the following subsections and the base of the FOM will be explained here.

The FOM technique is the idea of forcing a sinusoidal motion (5) on the body with an actuator, that can define the motion with an amplitude and a frequency. With this technique it is possible to characterize the disk inertia and damping properties in a wide range of conditions. Then, using a spring-mass system description the linear equation of a body subjected to a FOM, for a single degree of freedom (Dof) z is:

$$(m + a)\ddot{z} + b\dot{z} + cz = F_h + F_k + F_I, \quad (4)$$

$$z = z_a \sin(\omega t), \quad (5)$$

Where, z is the motion of the body, $\dot{z}$ is the velocity and $\ddot{z}$ is the acceleration of the body. ω the frequency of motion, m is the body mass and c is the hydrodynamic restoring coefficient that represent the stiffness of the spring system. As a consequence of the motion, z, different forces are generated. F_h is the measured hydrodynamic force, which is the sum of forces developed by the flow-structure interaction (dynamic pressure and the tangential viscous forces). The hydrostatic forces F_k, are developed by the water pressure and are described as $F_k = \rho g h$, where h is the distance from the measured point to the free surface, which in a FOM vary on time. These forces, are subtracted from the total measured force (experimental tests) or simply not measured in the numerical simulation. The inertial forces, F_I, in this numerical setup are zero, due to the lack of mass on the body. Then, using the sinusoidal form of the measured force, F_h, Equation 4, can be rewritten as:

$$a\ddot{z} + b\dot{z} = F_1 \sin(\omega t + \varepsilon), \tag{6}$$

Then, two different methods can be applied to obtain the values of the added mass and the viscous damping coefficient. The first option is described by Greaves & Iglesias (2018), which is directly derived from the equations 4 and 5. However, in this work the method described by T. Sarpkaya & Isaacson (1981), is applied to find the drag coefficient (Eq. 7) and the added mass (Eq. 8). Then, with the Fourier relations described by Tao & Dray (2008) in equation 9, we can obtain the linear viscous damping coefficient for heave motion.

$$C_d = \frac{3}{4\rho S_d z_a \omega} \int_0^T F_h(t) \cos(\omega t) dt, \tag{7}$$

$$a_{33} = \frac{1}{\pi \omega z_a} \int_0^T F_h(t) \sin(\omega t) dt, \tag{8}$$

$$b_{33} = \frac{1}{3} \mu \beta C_d D_d KC, \tag{9}$$

where, T is the period of motion, S_d the area of the disk.

With a similar process, it is possible to determine the a_{55} and b_{55} values for rotational motion. Then, a_{55} is the added moment of inertia and no longer the added mass. Also, note that these parameters are described with the sub index 55, which correspond to pitch motion, but in a symmetrical system, it would also be equivalent for roll motion.

$$a_{55} = \frac{1}{\pi \omega \theta_a} \int_0^T M_h(t) \sin(\omega t) dt\ , \tag{10}$$

$$b_{55} = \frac{1}{\pi \theta_a} \int_0^T M_h(t) \cos(\omega t) dt, \tag{11}$$

where, the θ_a represent the angular amplitude of motion and M_h the hydrodynamic moment of inertia.

The M_h moment is the result of the product of the distance square from the centre of rotation to the force point of action, by the F_h forces previously mentioned. The centre of rotation is commonly associated to the centre of gravity and the point of action will be assumed as the centre of the disk. However, in this case, due to the nature of the methodology is assumed to be at the free surface with a specific position on the x - y plane.

2.2 *Computational Fluid dynamic*

The CFD simulations in this work are performed using the standerd `interFoam` solver from the open-source libraries of OpenFOAM. `interFoam` solves the Reynolds-Averaged Navier-Stokes (RANS) equations for two incompressible, isothermal and immiscible fluids, using a Volume of Fluid (VoF) phase-fraction based interface capturing approach. It is described in the following equations:

$$\frac{\partial(\rho \boldsymbol{u})}{\partial t} + \nabla \cdot (\rho \boldsymbol{u}\boldsymbol{u}) = -\nabla p + \nabla^2(\mu \boldsymbol{u}) + \rho g + F_t, \tag{12}$$

$$\nabla \cdot \boldsymbol{u} = 0, \tag{13}$$

where, $\boldsymbol{u} = (u, v, w)$ is the fluid velocity, p the flow pressure, μ is the dynamic viscosity and g the gravity acceleration constant.

This equation is comprised of six terms that represent (from left to right) the following contributions; the partial time derivative, the convective term, pressure gradient, diffusion term, gravity term and the Reynolds stress or the turbulent term. This last term is added by the selected turbulence model k-ωSST.

2.3 *Boundary Element Method*

The frequency domain analysis was carried out in the open-source BEM potential flow code NEMOH. Which will be used to calculate the added mass properties for each frequency of the desired geometry. The governing equations for this code are the continuity (14) and Lagrange equations (15), that are generated by assuming different flow hypothesis (G. Delhommeau, 1993).

$$\nabla^2 \Phi = 0, \tag{14}$$

$$\frac{p}{\rho} + g x_3 + \frac{\boldsymbol{u}^2}{2} + \frac{\partial \Phi}{\partial t} = F(t), \tag{15}$$

where, x_3 represents the vertical axis and Φ is the velocity potential function.

3 FREQUENCY DOMAIN ANALYSIS

A study of different heave plate shapes was carried out, with two purposes. First, to understand the effects on the added mass and added moment of inertia by changing the shapes gradually. Secondly, to understand and compare how the potential code would solve the proposed non-conventional shapes. The last, is critical in a future optimization process of the system with emphasis on the disks, with the option of using this potential tool. Furthermore, the comparison with the CFD FOM tests can answer how well the potential flow code can identify changes in the added mass effects.

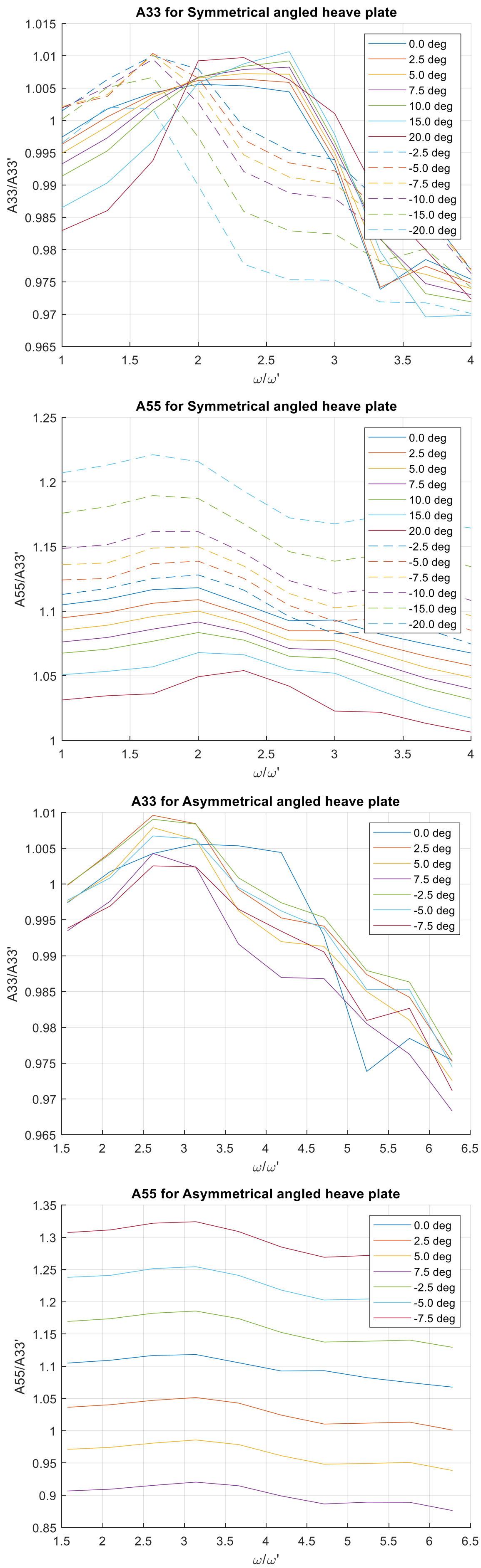

Figure 1. The added mass properties of different proposed geometries are shown, all in a non-dimensional form. From top to bottom (a-d), symmetrical angled disk heave and pitch, asymmetrical angled disk heave and pitch.

The analysis was carried out with the geometry used in Lopez-Pavon & Souto-Iglesias (2015) to obtain control data (Figure 4.). Then, angled disks were designed, maintaining the main dimensions of the original geometry; column diameter, heave plate diameter and location. Here, two modes of motion were analysed, heave and pitch. Furthermore, two variations of pitch motion were used. First, a rotation calculated around a centre of rotation (CoR) located at a point at the centre axis of the body (here, the free surface level was used). Secondly, a pitch motion calculated around a CoR in an external point, as a representation of a whole semi-submersible platform, here a point one metre further from the centre of the axis was used (Figure 4). In that way, moments and forces are easier to compare. The proposed angled disk are classified as symmetrical and asymmetrical geometries (Figure 2). In the first case, the disk is angled as a hollow cone in the positive or the negative direction. In the case of the asymmetrical geometries, flat disks are angled with respect of the main axis of the column, again in positive and negative direction.

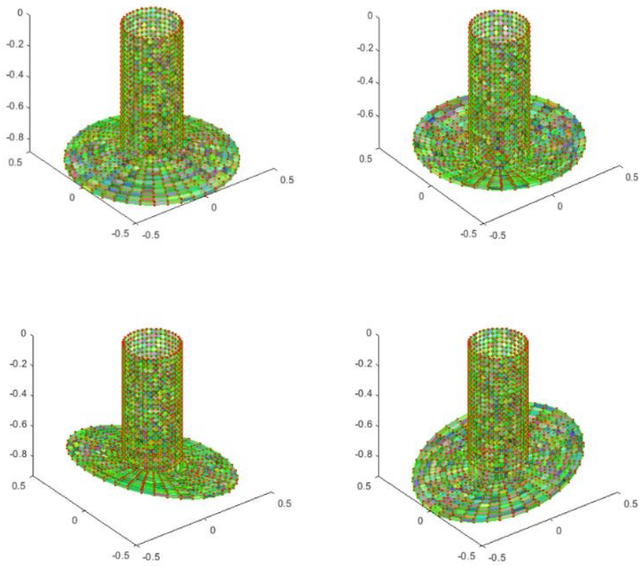

Figure 2. From left to right and top to bottom, symmetrical positive and negative angled disk. Asymmetrical positive and negative angled disk.

In general, it was observed that for heave motion, the added mass did not vary significantly with the proposed geometries. That, at an initial stage of this research seems logical, due to the constant projected area of the heave plate, related to the approximated theoretical added mass of a disk explained by Zhu & Lim (2017). In case of the added moment of inertia, there is an important increment on the values in the asymmetrical and symmetrical angled disks. This is attributable to the increasing projected area of the disk as the angle increases. However, only one of the angled directions creates an increment in the added moment of inertia compared with the control conventional geometry (Figure 1.d). In the case of the symmetrical geometry, there is also a difference on the added mass generated by a positive and a negative angled disk. Both of them can generate more added mass by having a larger projected area. However, the positive angled geometry, have a shorter lever to the CoR and the moment of inertia is therefore, reduced. On the contrary, the negative angled disk, increase the distance to the CoR and therefore the total moment of inertia. However, the effect of the direction of the hollow cone on the added mass is not jet understood.

3.1 *Motion decomposition*

In order to simplify and isolate effects, a single column-disk was selected for the study. However, it is also possible to decompose the pitch motion of a single column of a platform. The motion of the platform can be thought of as the sum of the effects of each column (neglecting the coupling effects), and the pitch motion of a single column can be described by a rotation around an external point. Then, a possible approximation for a rotation around an external CoR, it could be the sum of a translational and a purely rotational motion. Furthermore, these two modes of motion together would develop the added moment of inertia. This approach makes sense when a potential flow solver is being use, where there is not free-surface and effects are calculated linearly. However, this may not be always true, especially when complex flow phenomena are occurring around the disk. This highlights the necessity of a study with complex flow that can model the flow-structure interaction, to generate better understanding of this kind of motion.

Therefore, if we can consider a rotational motion from an external point, to be equal to the sum of a translational and rotational motion. It is possible to assume that disk-developed effects in the different modes of motion can be decomposed in the same way. To prove this, in Figure 3, a comparison of the added moment of inertia for pitch from an external point is made against the sum of the heave added mass by the lever squared and the pitch added moment of inertia, with the rotational point in the centre of the column. Here, the geometry of the conventional heave plate was used. As can be seen, the results are similar, proving that this approximation can be used for this application. However, it was observed that with a long arm of rotation minor differences appear. In addition, the geometry must be symmetrical for this to be true with the data calculated by NEMOH.

With this kind of analysis and approximations, it is easy to understand that as the platform gets wider, (with a higher overall radius or distance between the columns) the heave added mass of the column becomes the most significant for the whole platform rotation response. On the contrary, when the platform shrinks and especially if gets a deeper draft, the pitch added moment of inertia of the individual column gains a significant role on the added moment of inertia of the whole platform. Geometries like the symmetrical heave plates with negative angles, show significant increase in the added moment of inertia for an external point of rotation (Figure 1.b). This can be explained with the relatively small distance from the column to the CoR, compared with the draft, making the heave added mass less significant. However, these improvements also show that it is possible to increase the added moment of inertia of a platform by adding a significant pitch added moment of inertia of the individual disk-column system. Nevertheless, this also implies that these changes in the geometry do not affect the heave added mass produced by the disk. As shown in Figure 1.a, potential results are not significantly affected by these changes. This must be analysed with complex flow models for each new geometry, for instance, an effect might not be significant

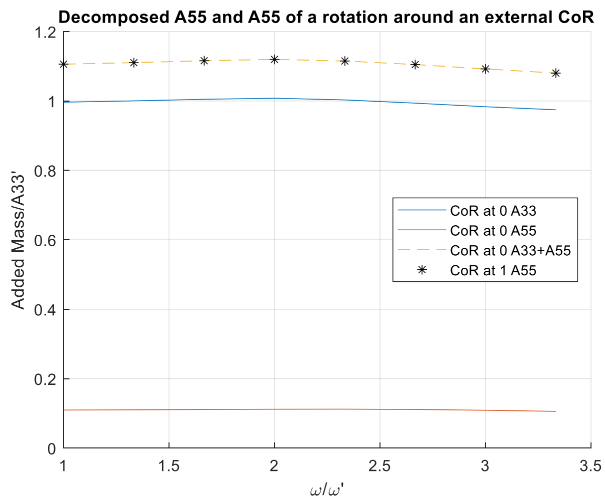

Figure 4. Added mass decomposition, based on the motion characteristics of a conventional disk.

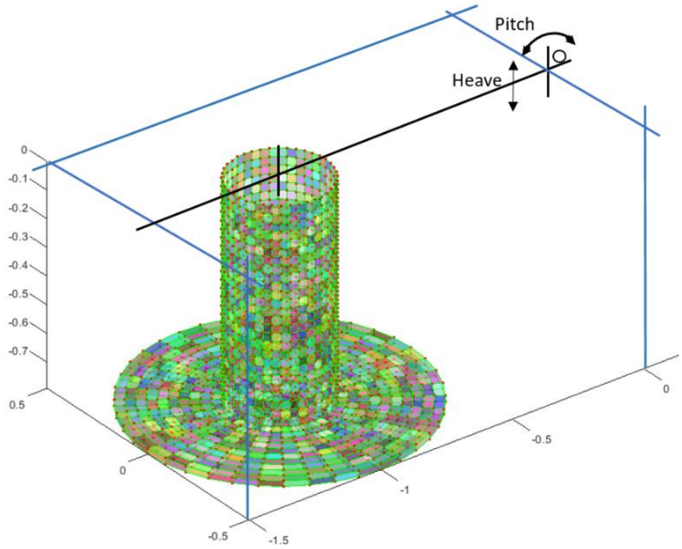

Figure 3. Heave plate obtained from Lopez-Pavon & Souto-Iglesias (2015), with a center of rotation displaced by 1 m in the x direction.

until the angle of the proposed plates goes above an unknown limit.

4 FORCED OSCILLATION ANALYSIS

A numerical study using a RANS CFD tool was carried out with the geometry used by (Lopez-Pavon & Souto-Iglesias, 2015) and one of the proposed non-conventional shapes. The objective was to obtain the added mass properties of these geometries and compare them against those obtained using the potential flow code. Furthermore, obtain the effective added mass properties and trends of the proposed non-conventional geometries, and in addition, to test the hypothesis of motion decomposition (Section 3.1) in a more complex flow-structure interaction. As explained in section 2.1, the FOM test can give us the inertia and damping properties developed by a disk under oscillating flow. This technique has some advantages over the conventional decay test. While a decay test experiences a single frequency during the motion (natural frequency), the FOM can change this parameter to any that might be of interest. In addition, as can be experienced with decay tests, the amplitude of oscillation or the drop height can generate large discrepancies, with FOM the amplitude can be varied with precision and a curve of the property versus KC can be described.

The simulation setup was made as a 3D domain with one symmetry plane, and then only half of the column-disk system is solved. The used mesh was generated with the cfMesh open-source tool, with 1.2-2 million cells. It is important to note that this mesh is much coarser than the commonly used for these applications, specifically for heave cases. This is because, for heave motion with two symmetry planes, it is possible to model only a section of the disk, i.e. 1 of the 360 degrees that compound a disk. However, this technique is not suitable for pitch motions.

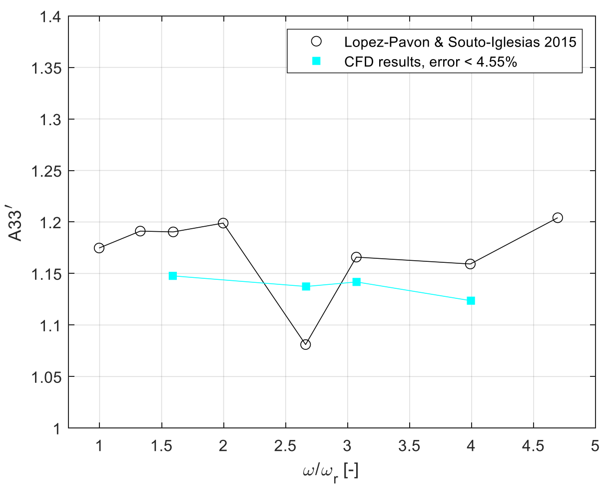

Figure 5.Comparison of the experimental FOM test data (Lopez-Pavon & Souto-Iglesias, 2015) and the obtained CFD results.

To validate the setup, the experimental FOM test from Lopez-Pavon & Souto-Iglesias (2015) was used. The compared cases are KC = 0.3 and ω/ω'=1.5-4. In Figure 5, is possible to see the good correlation achieved, even with a "coarse" mesh, achieving a maximum error of less than 5%.

In the inertia-dominated regime (KC < 5), the forces obtained by the FOM tests, are difficult to analyse, especially the drag force properties (T. Sarpkaya, 2010). This can generate some scattering of results for a single condition.

In addition, a basic mesh sensitivity analysis was done with the 2.67 ω/ω' case. This point was selected because it represents an off trend result that ideally must be identified by the model. In the Table 1, the main characteristics of the three compared meshes are shown. The differences of added mass from the used mesh (Mesh 1) and finer meshes are calculated, showing a minimal dependency of the mesh.

Table 1. Mesh sensitivity analysis

	Main cell size	Cells	Difference
	[m]	[millions]	[%]
Mesh 1	0.3	1.2	-
Mesh 2	0.25	1.8	0.69%
Mesh 3	0.175	3.9	0.82%

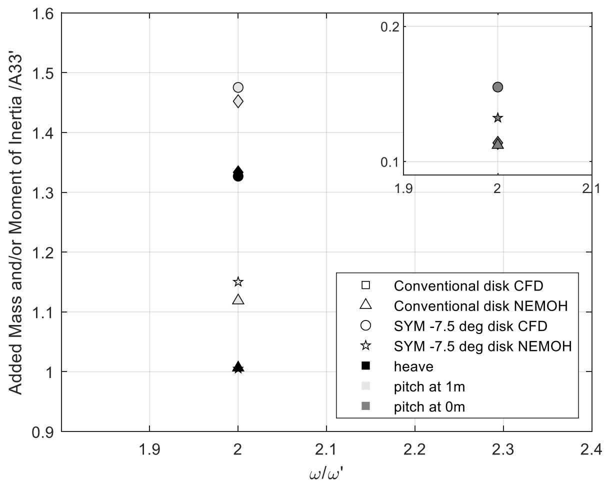

Figure 6. Comparison of the CFD and NEMOH added mass results for translational and rotational motion, with two rotational modes.

Figure 6, shows the results of the CFD forced oscillation motion modelling and the NEMOH results, of a conventional heave plate and a symmetrical angled plate (-7.5 deg). The results of this geometry are also shown in the Figure 1.a and 1.b. It can be observed that the non-linear CFD results have large differences with the potential results. Being consistent with what has been found for an oscillating-translational disk, in other studies (Lopez-Pavon & Souto-Iglesias, 2015; L. Tao et al., 2007; Longbin Tao & Dray, 2008). However, the trend showed by NEMOH is consistent, as the increase observed in the symmetrical -7.5deg angled disk compared with the conventional disk. It is important to mention that the differences between the conventional and one of the proposed geometries can vary with different angles, amplitudes and frequencies that have not been studied. For more consistent conclusions further work must be done.

The Figure 6, shows values of heave added mass and pitch added moment of inertia for a rotation on the centre of the column and a rotation on a point one metre farther in the *x* direction. Showing data for two geometries, a conventional heave plate and the symmetrical -7.5 deg angled plate. Both under the same forced conditions; $\omega/\omega' = 2$, an amplitude of 5 deg for the rotational tests and 0.0871 m for the translational motion. The translational amplitude is equivalent to the vertical dimension developed by a rotation of 5 deg with a 1 m long arm. Then, the KC can be calculated as usual for the translational motion, but in addition, a KC number is considered for the rotational motion from an external point (KC'). Being defined as:

$$KC' = \frac{2\pi \sin(\theta_a)\ell}{D_d}, \tag{16}$$

where, ℓ is the lever of rotation. In Figure 6, the lower values of the same case and method of calculation are the added mass and the higher values the added moment of inertia with a CoR in $x = 1$. In the inset at the top the added moment of inertia with a CoR of $x = 0$. As can be seen in the Figure 6, the hypothesis of decomposition of motion is still valid with the tested non-conventional disk, however, further research must be done to ensure that this will remain valid for different shapes and conditions. In Figure 6, it is possible to observe that the differences of the potential

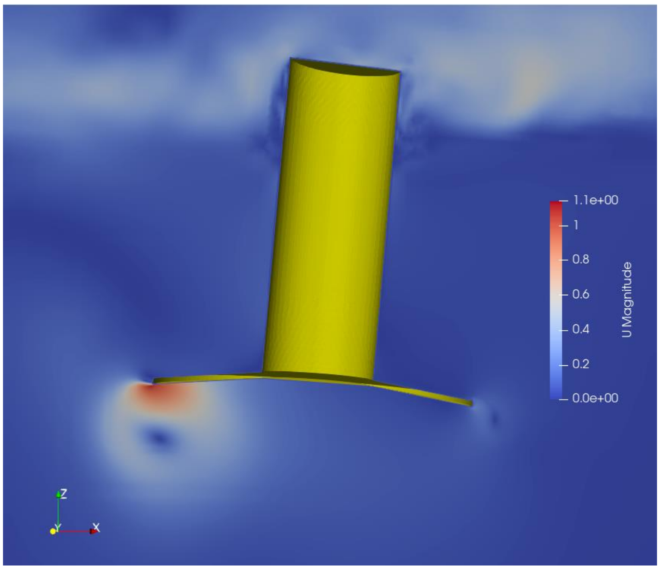

Figure 7. FOM from an external point test of the symmetrical -7.5 deg angled disk.

and the CFD results of the conventional disk are minimal, this can be attributed to the low flow-structure interaction occurring with that geometry. However, with the other geometry the small applied angle, can develop stronger flow-structure interaction resulting and a much bigger (in comparison) difference between the methods.

In the Figure 7, the FOM test for a rotation from an external point is shown. It is interesting to observe the strong vortex shedding that is created. Furthermore, the vortices are not symmetrical and they are developed with different magnitude depending on the position and the motion of the system, contrasting with the more studied translational vertical motion cases.

5 CONCLUSIONS AND FUTURE WORK

A numerical analysis with two different methods was done, with a main objective of study how motion reduction disks, for offshore application, behave under rotational motion. This was made with the BEM code NEMOH, used to compare heave and pitch added mass and their contribution for a complex pitch rotation. In addition, a CFD study was carried out by using a non conventional characterization technique for damping and inertia properties. Both results were compared and discussed, then the following outcomes were obtained:

- NEMOH underestimates the added mass effects for both heave and pitch motion of a column-disk system. However, with the tested geometries it finds the qualitative differences between them, showing the correct trend observed in the symmetrical angled plate.
- The CFD setup can model with good agreement the added mass effects of a disk in different conditions.
- The motion decomposition approximation works well for the used geometries and methods. This technique helps to minimize the interference of effects when a detailed analysis is desired, being useful to improve specifics characteristics of a combined motion as a rotation from an external point.
- A minimum increase is observed with the proposed non-conventional disk with no significant decrement in the heave added mass. This case opens the possibility of a more optimal design and therefore more work needed to be undertaken.
- There is likely to be a configuration of position, dimensions and shapes more adequate for a semi-submersible FOWT application (depending on the pre-existing conditions). Furthermore, the distances from the added mass point of action of the different disk shapes to

the CoR, gain a major role being an alternative for different platform designs.
- More work must be done to analyse the effects of the asymmetrical vortex generation and how the prescribed conditions affect it.
- Further work is needed to understand how other characteristics of the platform will be affected by the presence of this non-conventional disk in translational and rotational motions. For instance, the viscous damping and wave excitation forces.

6 REFERENCES

Bayati, I., Jonkman, J., Robertson, A., & Platt, A. (2014). The effects of second-order hydrodynamics on a semisubmersible floating offshore wind turbine. *Journal of Physics: Conference Series*, *524*(1). https://doi.org/10.1088/1742-6596/524/1/012094

G. Delhommeau. (1993). Seakeeping codes AQUADYN and AQUAPLUS. *Numerical Simulation of Hydrodynarnics : Ships and Offshore Structures ECOLE Centrale Nantes*.

Garbis H. Keulegan, & Carpenter, L. H. (1958). Forces on Cylinders and Plates in an Oscillating Fluid. *Journal of Research of the National Bureou of Standars*.

Greaves, D., & Iglesias, G. (2018). *Waves and Tidal Energy* (John Wiley & Sons Ltd (ed.); first edit).

James, R., & Costa Ros, M. (2015). Floating Offshore Wind : Market and Technology Review. *Carbon Trust*, *June*, 1–168. http://www.carbontrust.com/media/670664/floating-offshore-wind-market-technology-review.pdf

Journee, J., & Massie, W. (2000). *ffshore hydromechanics* (first edit). CITG Section Hydraulic Engineering (<2005).

Lerch, M., De-Prada-Gil, M., Molins, C., & Benveniste, G. (2018). Sensitivity analysis on the levelized cost of energy for floating offshore wind farms. *Sustainable Energy Technologies and Assessments*, *30*, 77–90. https://doi.org/10.1016/J.SETA.2018.09.005

Lopez-Pavon, C., & Souto-Iglesias, A. (2015). Hydrodynamic coefficients and pressure loads on heave plates for semi-submersible floating offshore wind turbines: A comparative analysis using large scale models. *Renewable Energy*, *81*, 864–881. https://doi.org/10.1016/j.renene.2015.04.003

Maimon, A. – D. (2019). Brief review about floating offshore wind turbines projects. *Analele Universităţii 'Dunărea de Jos' Din Galaţi. Fascicula XI, Construcţii Navale/ Annals of 'Dunărea de Jos' of Galati, Fascicle XI, Shipbuilding*, *41*, 49–62. https://doi.org/10.35219/annugalshipbuilding.2018.41.08

Myhr, A., Bjerkseter, C., Ågotnes, A., & Nygaard, T. A. (2014). Levelised cost of energy for offshore floating wind turbines in a lifecycle perspective. *Renewable Energy*, *66*, 714–728. https://doi.org/10.1016/j.renene.2014.01.017

Roald, L., Jonkman, J., Robertson, A., & Chokani, N. (2013). The effect of second-order hydrodynamics on floating offshore wind turbines. *Energy Procedia*, *35*, 253–264. https://doi.org/10.1016/j.egypro.2013.07.178

T. Sarpkaya. (2010). *WAVE FORCES ON OFFSHORE STRUCTURES*. Cambridge University Press.

T. Sarpkaya, & Isaacson., M. (1981). *Mechanics of Wave Forces on Offshore Structures*. Van Nostrand Reinhold.

Tao, L., Molin, B., Scolan, Y. M., & Thiagarajan, K. (2007). Spacing effects on hydrodynamics of heave plates on offshore structures. *Journal of Fluids and Structures*, *23*(8), 1119–1136. https://doi.org/10.1016/j.jfluidstructs.2007.03.004

Tao, Longbin, & Dray, D. (2008). Hydrodynamic performance of solid and porous heave plates. *Ocean Engineering*, *35*(10), 1006–1014. https://doi.org/10.1016/j.oceaneng.2008.03.003

Zhu, L., & Lim, H. C. (2017). Hydrodynamic characteristics of a separated heave plate mounted at a vertical circular cylinder. *Ocean Engineering*, *131*(April 2016), 213–223. https://doi.org/10.1016/j.oceaneng.2017.01.007